The EMBO Journal Vol.19 No.4 pp.562–571, 2000

A truncated isoform of the PP2A B56 subunit promotes cell motility through paxillin phosphorylation

Akihiko Ito, Tatsuki R.Kataoka, Masafumi Watanabe[1], Kazutaka Nishiyama[2], Yuichi Mazaki[3], Hisataka Sabe[3,4], Yukihiko Kitamura and Hiroshi Nojima[2,5]

Department of Pathology, Medical School and [2]Department of Molecular Genetics, Research Institute for Microbial Diseases, Osaka University, Suita, Osaka 565-0871, [1]Medical and Biological Laboratories (MBL), Ina, Nagano 396-0002, [3]Department of Molecular Biology, Osaka Bioscience Institute, Suita, Osaka 565-0874 and [4]Graduate School of Biostudies, Kyoto University, Sakyoku, Kyoto 606-8502, Japan

[5]Corresponding author
e-mail: hnojima@biken.osaka-u.ac.jp

Both F10 and BL6 sublines of B16 mouse melanoma cells are metastatic after intravenous injection, but only BL6 cells are metastatic after subcutaneous injection. Retrotransposon insertion was found to produce an N-terminally truncated form (Δγ1) of the B56γ1 regulatory subunit isoform of protein phosphatase (PP) 2A in BL6 cells, but not in F10 cells. We found an interaction of paxillin with PP2A C and B56γ subunits by co-immunoprecipitation. B56γ1 co-localized with paxillin at focal adhesions, suggesting a role for this isoform in targeting PP2A to paxillin. In this regard, Δγ1 behaved similarly to B56γ1. However, the Δγ1-containing PP2A heterotrimer was insufficient for the dephosphorylation of paxillin. Transfection with Δγ1 enhanced paxillin phosphorylation on serine residues and recruitment into focal adhesions, and cell spreading with an actin network. In addition, Δγ1 rendered F10 cells as highly metastatic as BL6 cells. These results suggest that mutations in PP2A regulatory subunits may cause malignant progression.

Keywords: cytoskeleton/invasion/protein phosphatase/subtraction/targeting subunit

Introduction

B16 mouse melanoma cells were originally established from a *de novo* melanoma tumor. The F1 and F10 sublines were obtained through one and 10 rounds of *in vivo* selection of B16 cells, respectively. BL6 cells were obtained through six rounds of *in vitro* selection of F10 cells (Poste *et al*., 1980). The metastatic potentials increase as the number of rounds of selection increases. The BL6 subline is metastatic to lungs after both intravenous and subcutaneous injection, whereas the F10 subline is metastatic to lungs only after intravenous injection. The genetic differences between these sublines have been investigated in an attempt to identify novel genes that may promote or suppress metastasis. We found a prominent induction of expression in BL6 cells of the gene encoding the protein phosphatase type 2A (PP2A) B56γ regulatory subunit.

PP2A is an intracellular serine/threonine protein phosphatase that regulates a variety of cellular processes, including signal transduction, cell cycle progression and development (reviewed in Shenolikar, 1994; Wera and Hemmings, 1995). PP2A holoenzymes consist of a common dimeric core of invariable catalytic (C) and structural (A) subunits associated with a variable regulatory (B) subunit (Usui *et al*., 1988). To date, three unrelated families of PP2A regulatory subunits have been identified, denoted PR55 (or simply B), B56 (B′) and PR72 (B″). Five distinct mammalian genes encode members of the B56 subunit family, and at least 13 isoforms are generated from these genes (McCright *et al*., 1996; Tehrani *et al*., 1996). The B56γ subunit includes three alternative splicing variants, B56γ1, B56γ2 and B56γ3 (Figure 1B). The signal transduction pathway via mitogen-activated protein (MAP) kinase triggers cell proliferation and differentiation in response to various growth factors. MAP kinase becomes activated after being phosphorylated on tyrosine and threonine residues. PP2A is a major phosphatase that inactivates MAP kinase by dephosphorylating these residues (Alessi *et al*., 1995). PP2A also plays an essential role in regulating the cell cycle processes, such as the spindle checkpoint, during M-phase progression in yeast and *Xenopus* oocytes (reviewed in Millward *et al*., 1999). A similar role for PP2A has been postulated in mammalian cells. Okadaic acid (OA), an inhibitor of PP2A, promotes mitosis in G_2-arrested hamster fibroblasts (Yamashita *et al*., 1990). Hox11 interacts with the PP2A C subunit and disrupts the G_2/M cell cycle checkpoint in human T cells (Kawabe *et al*., 1997). Since the association between PP2A and microtubules is regulated during the cell cycle, it has been proposed that PP2A regulates cell cycle-dependent microtubule functions, such as karyokinesis and membrane transport (Sontag *et al*., 1995).

Invasion into surrounding tissues occurs as a result of cell movement through cellular and extracellular matrix barriers into neighboring sites (reviewed in Liotta *et al*., 1991). To invade, cells alter their cell–cell and cell–extracellular matrix interactions, and remodeling of the extracellular matrix occurs. In addition, reorganization of the cytoskeleton and increased cell motility are required. Integrin-mediated focal adhesions (FA) serve as a bridge between these extracellular and intracellular events (reviewed in Burridge and Chrzanowska-Wodnicka, 1996). The cytoplasmic domains of integrins are linked to cytoskeletal actin, probably through cytoplasmic structural molecules, such as vinculin, talin and α-actinin. Other proteins participating in FA are categorized as regulatory molecules, including focal adhesion tyrosine kinase (FAK) and paxillin. Paxillin is a multidomain-containing adaptor molecule that provides binding sites for various proteins

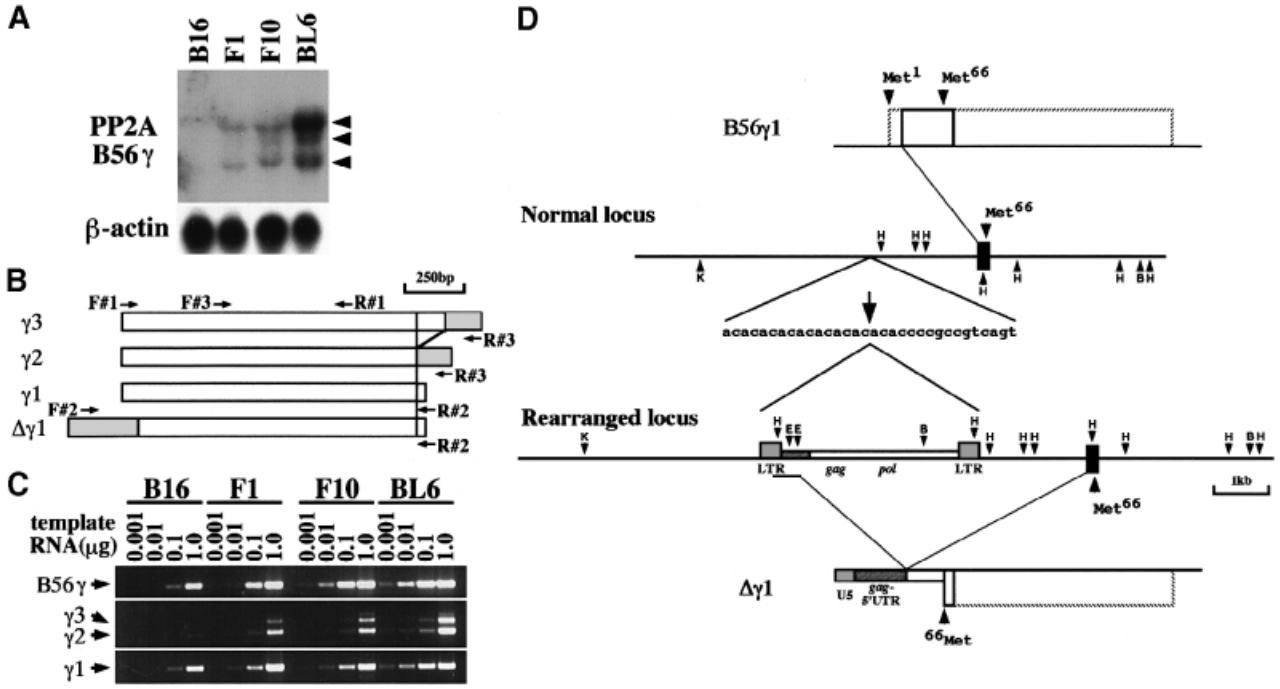

Fig. 1. PP2A B56γ gene expression in B16 sublines. (**A**) PP2A B56γ mRNA expression in four types of B16 melanoma cells. A 5 μg aliquot of total RNA per lane was blotted on nylon membrane and hybridized with PP2A B56γ cDNA probe. Three transcripts were detected at 2.1, 3.8 and 4.4 kb (indicated by arrowheads). Reprobing with β-actin probe verified equal RNA loading. (**B**) Schematic diagram of the B56γ subunit cDNA for the three isoforms, γ3, γ2 and γ1, generated by 3′-terminal alternative splicing. The Δγ1 cDNA was generated by a fusion of the IAP sequence (gray box) with the B56γ1 cDNA. Sense (F#1, F#2 and F#3) and antisense (R#1, R#2 and R#3) oligonucleotide primers used in the present study are indicated by arrows. (**C**) Detection of the three B56γ isoforms by RT–PCR. Various amounts (0.001, 0.01, 0.1 and 1.0 μg) of total RNA were reverse-transcribed and amplified by PCR. Primer sets used were: F#3 and R#1 to detect the region common to all B56γ isoforms (upper panel); F#3 and R#3 specific for B56γ3 (longer PCR products) and γ2 (shorter PCR products) (middle panel); and F#3 and R#2 specific for B56γ1 (lower panel). In the upper panel, a gradual increase in band intensity from B16 to BL6 cells correlates well with the result of Northern blot analysis (A), indicating the semiquantitative nature of this analysis. (**D**) Genomic and cDNA organization of the PP2A B56γ gene in BL6 cells. A part of the PP2A B56γ gene locus cloned in the present study is shown as two lines in the middle. One exon (black boxes) was included. It encoded nucleotides 44–242 of the B56γ1 cDNA, in which the second methionine (Met66) was present. One allele was rearranged by insertion of an IAP sequence that consists of *gag* and *pol* elements flanked by the LTR. The insertion site, indicated by an arrow, was located within an AC-repeat region 2.2 kb upstream of the exon. B56γ1 (upper box) and Δγ1 (lower box) cDNA sequences transcribed from the genomic region shown in the middle are outlined with solid lines. Full-length reading frames for B56γ1 and Δγ1 are outlined with broken lines. Restriction sites: B, *Bam*HI; E, *Eco*RI; H, *Hin*dIII; K, *Kpn*I.

at the FA. The paxillin N-terminus, composed of five LD motifs, contains binding sites for the non-receptor kinases FAK, Csk and Src, and the structural protein vinculin (Sabe *et al*., 1994; Turner and Miller, 1994). On the basis of such an adaptor function and its propensity to become phosphorylated in response to cell adhesion, paxillin has been implicated in the regulation of FA assembly (Burridge *et al*., 1992). On the other hand, the C-terminus, composed of four LIM domains, is involved in determining paxillin subcellular localization (Brown *et al*., 1996). Recent reports indicate that serine and threonine phosphorylation of the paxillin LIM domains is required for paxillin targeting to nascent FA (Brown *et al*., 1998). Additionally, serine/threonine kinase activity has been observed to localize physically with paxillin (Bellis *et al*., 1997). Further, it has been reported that several serine/threonine kinases including the β1-integrin-binding kinase ILK, p21-activated kinase (PAK) and $p190^{ROK\alpha}$ localize to FA (Hannigan *et al*., 1996; Harden *et al*., 1996; Leung *et al*., 1996). However, mechanisms for the reversal of serine/threonine phosphorylation at FA deserve more intensive study.

In the present study, we found an interaction of paxillin with PP2A C and B56γ subunits by immunoprecipitation (IP). Immunofluorescence (IF) demonstrated the subcellular localization of the B56γ1 isoform at FA. These results suggested that this isoform directed the PP2A AC dimer to FA, and that the B56γ1-containing PP2A heterotrimer was implicated in the paxillin phosphorylation state. In BL6 cells, retrotransposon insertion was found in one locus of the gene encoding the B56γ subunit. This mutated locus produced an N-terminally truncated form of the B56γ1 isoform, termed Δγ1. Δγ1 behaved similarly to B56γ1 in targeting the PP2A AC dimer to paxillin. However, Δγ1 caused constitutive paxillin phosphorylation on serine residues, probably due to a failure of the Δγ1-containing PP2A heterotrimer to dephosphorylate paxillin. Interestingly, Δγ1 also promoted NIH 3T3 (3T3) cell migration *in vitro* and F10 cell metastasis to lymph nodes. Δγ1 recruitment into FA might disrupt a balance between phosphorylation and dephosphorylation activities that modulate protein assembly at FA.

Results

PP2A B56γ gene expression in BL6 cells

While examining the difference in gene expression levels between F10 and BL6 cells by the cDNA subtraction method, we found that the PP2A B56γ gene showed the

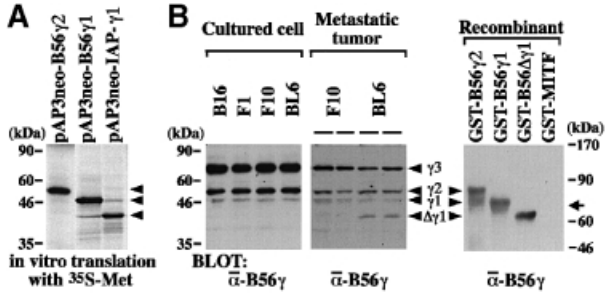

Fig. 2. Detection of Δγ1 protein. (**A**) *In vitro* translation of the chimeric cDNA transcribed from the rearranged locus of the PP2A B56γ gene. The three constructs indicated were transcribed and translated in the presence of [^{35}S]methionine. Products were separated by SDS–PAGE and autoradiographed. Three arrowheads indicate the position of B56γ2 (upper), γ1 (middle) and Δγ1 (lower). (**B**) Δγ1 protein expression in BL6 cells. Cell lysates (50 μg) of cultured melanoma cells were blotted (left panel). In the spontaneous metastasis assay, F10 and BL6 cells metastasized into popliteal lymph nodes at an incidence of ~30% (see Figure 8B). The metastatic lesions formed in the lymph nodes were excised at amputation, lysed and blotted (middle panel). In the right panel, recombinant B56γ2, γ1 and Δγ1 proteins were blotted. GST–MITF was blotted as an unrelated protein (Ito *et al.*, 1998). The faster migrating molecule in the lane of GST–B56γ2 may be due to degradation. The blots were detected with anti-B56γ Ab. Arrowheads indicate three B56γ isoforms and Δγ1. The arrow on the right indicates the position of GST–MITF migration.

highest induction of expression in BL6 cells (Figure 1A). RT–PCR analysis revealed that the increase in mRNA levels was most apparent for the B56γ1 isoform among the three isoforms (Figure 1C). In a BL6 cDNA library, we found a clone carrying a chimeric cDNA, termed pAP3neo-IAP-γ1, in which the sequence upstream of nucleotide 43 of the B56γ1 isoform (Tehrani *et al.*, 1996) was replaced by part of the sequence of an intracisternal type A particle (IAP) (Figure 1D). The 5′-terminal sequence corresponded to the U5 region of the long terminal repeat (LTR), and was followed by the 5′-untranslated region (UTR) of the *gag* element (Figure 1D). RT–PCR demonstrated that the replacement occurred only in the B56γ1 isoform but not in the B56γ2 or B56γ3 isoform, and that the chimeric mRNA was five times as abundant as the normal B56γ1 mRNA in BL6 cells (data not shown). The genomic structure of the PP2A B56γ locus was determined in BL6 cells (Figure 1D). In one allele, the IAP sequence was inserted within an AC-repeat region 2.2 kb upstream of an exon encompassing nucleotides 44–242 of the B56γ1 cDNA (Figure 1D). The insertion was flanked by an imperfect 6 bp target site duplication (ACACAC/ACACCC), a typical feature of IAP transposition events (Kuff and Lueders, 1988).

The chimeric transcript from the rearranged locus lacked the original translation start codon of the B56γ1 isoform. When pAP3neo-IAP-γ1 was transcribed and translated *in vitro*, the product was detected as a band of ~40 kDa (Figure 2A). Translation appeared to start from the second methionine (Met66) of the B56γ1 isoform. We termed this truncated protein variant Δγ1. Anti-B56γ antibody (Ab) specifically recognized recombinant B56γ2, γ1 and Δγ1 proteins (Figure 2B). Under the standard culture conditions, the B16 parent cells and their three sublines equally expressed the three isoforms of the B56γ subunit (Figure 2B). Despite the abundance of the chimeric transcript, Δγ1 protein expression was below the detection limit in cultured BL6 cells (Figure 2B). On the other hand, Δγ1 protein was detected in the tumors produced by lymphatic metastasis of BL6 cells but not of F10 cells (Figure 2B). The expression level for Δγ1 was higher than that for B56γ1 in the metastatic tumors of BL6 cells.

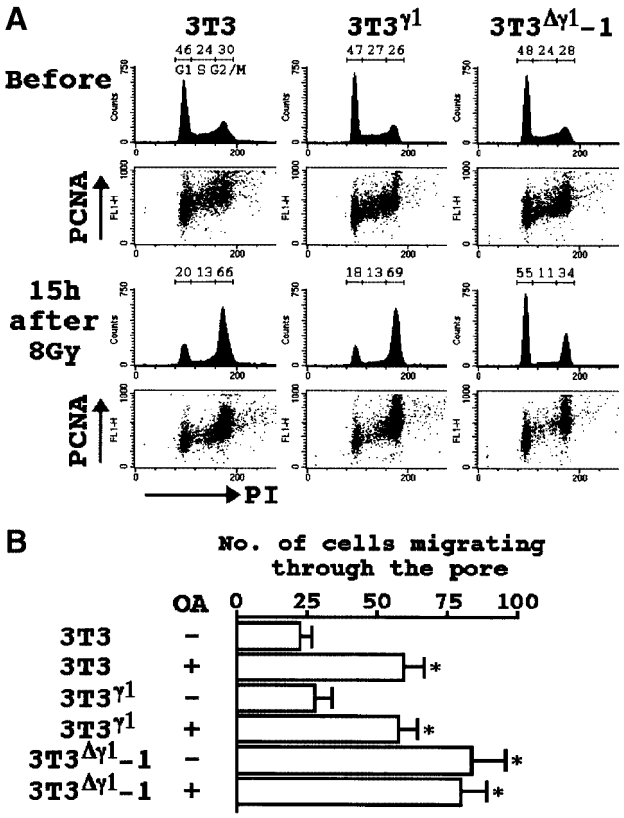

Fig. 3. Alteration of PP2A function by Δγ1. (**A**) Disruption of the G_2/M cell cycle checkpoint in 3T3$^{\Delta\gamma1}$ cells. Before and 15 h after the irradiation, cells were examined for DNA content (PI) and PCNA expression. Proportions (%) of cells resident in the G_1, S or G_2/M phase of the cell cycle are shown at the top of the histograms. (**B**) Cell migration assay in the presence or absence of OA (100 nM). The data represent the mean values (± SE) of three experiments. *P <0.05 by t-test when compared with the two values not denoted by asterisks.

Alteration of cell cycle and migration by Δγ1

We introduced either pAP3neo containing full-length cDNA for B56γ1 (pAP3neo-B56γ1) or pAP3neo-IAP-γ1 into 3T3 cells, and obtained three G418-resistant clones designated 3T3$^{\gamma1}$, 3T3$^{\Delta\gamma1}$-1 and 3T3$^{\Delta\gamma1}$-2. 3T3$^{\Delta\gamma1}$-1 and 3T3$^{\Delta\gamma1}$-2 yielded essentially identical results in the following experiments. The Δγ1 protein expression was detectable in 3T3$^{\Delta\gamma1}$-1 cells under the standard culture conditions (Figure 6B). There was no difference in the total cellular, cytoplasmic or nuclear PP2A activity between 3T3, 3T3$^{\gamma1}$ and 3T3$^{\Delta\gamma1}$-1 cells (data not shown). Nonetheless, the G_2/M cell cycle checkpoint was disrupted in 3T3$^{\Delta\gamma1}$-1 cells. After γ-irradiation, 3T3 and 3T3$^{\gamma1}$ cells were accumulated at G_2, whereas most of the 3T3$^{\Delta\gamma1}$-1 cells were arrested at G_1 but not at G_2 (Figure 3A). The total cellular levels of proliferating cell nuclear antigen (PCNA) during the cell cycle were comparable between these three types of cells both before and after irradiation (Figure 3A).

OA has been shown to render living cells more motile and rounded with reduced cytoskeletal organization (Young *et al.*, 1993; Maier *et al.*, 1995; Farve *et al.*,

1997). Consistently, we observed a 2-fold increase in the migratory ability of 3T3 cells after OA treatment (Figure 3B). A similar increase was observed in $3T3^{\Delta\gamma1}$-1 cells even without OA treatment (Figure 3B), further suggesting that Δγ1 blocked the function of PP2A.

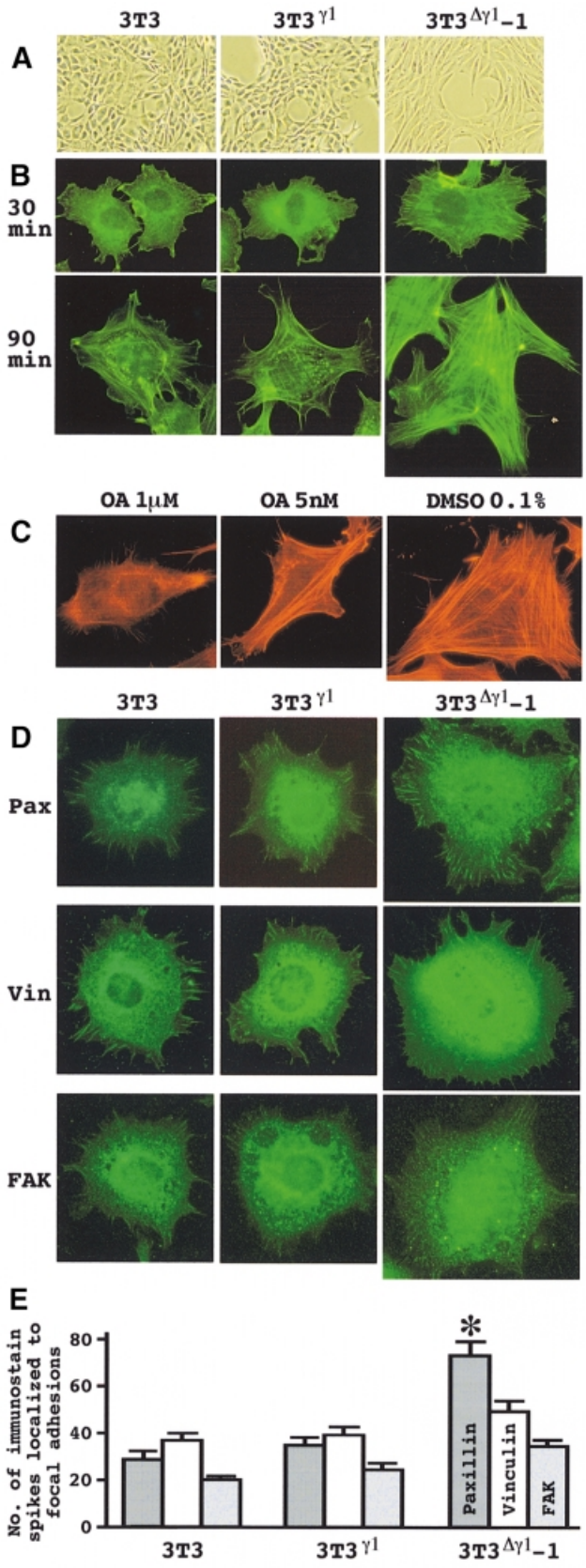

Cytoskeletal modulation by Δγ1

The effect of Δγ1 on cell morphology was the opposite to that of OA. $3T3^{\Delta\gamma1}$-1 cells were quite flat and well spread out, while $3T3^{\gamma1}$ cells did not show any morphological changes (Figure 4A). When the cells were seeded on fibronectin (FN), $3T3^{\Delta\gamma1}$-1 cells spread more rapidly than the other two types of cells (Figure 4B). Moreover, actin stress fibers were detected earlier and the networks were much better developed across $3T3^{\Delta\gamma1}$-1 cells (Figure 4B). OA interfered with the cytoskeletal elaboration even in $3T3^{\Delta\gamma1}$-1 cells. The lamellipodia were shrunk and the filamentous actin structure became less homologous (Figure 4C).

Accelerated spreading of $3T3^{\Delta\gamma1}$-1 cells on FN suggested that the cells could form FA more efficiently. Transfection with Δγ1 did not alter the recruitment of FAK and vinculin to nascent FA and their expression levels (Figures 4D and 5A). In contrast, paxillin was expressed prominently and localized efficiently to nascent FA at the early stage of $3T3^{\Delta\gamma1}$-1 cell contact (Figure 4D and E). Δγ1 might affect paxillin dynamics specifically during cytoskeletal organization.

Enhanced paxillin phosphorylation of serine residues in $3T3^{\Delta\gamma1}$ cells

We examined the induction of paxillin phosphorylation during the process of cell adhesion to FN. The cells were maintained in suspension for 30 min and subsequently allowed to attach and spread on FN. Attachment of 3T3 and $3T3^{\gamma1}$ cells to FN induced paxillin phosphorylation, which reached a maximum at 30 min and declined towards 90 min (Figure 5A). In contrast, paxillin was phosphorylated even in suspended $3T3^{\Delta\gamma1}$-1 cells, and the level of phosphorylation was much higher than in the other two types of cells plated on FN. Paxillin phosphorylation in $3T3^{\Delta\gamma1}$-1 cells was increased further by attachment to FN. We examined the degree of tyrosine phosphorylation and found that it was faint in suspension, but drastically increased after cells were plated on FN (Figure 5A). The profiles of tyrosine phosphorylation were comparable between 3T3, $3T3^{\gamma1}$ and $3T3^{\Delta\gamma1}$-1 cells. Phosphoamino acid analysis clearly demonstrated that paxillin was phosphorylated exclusively on serine, but only faintly on

Fig. 4. Δγ1 modulation of cell morphology. (**A**) Phase contrast images of cells on culture dishes. Note the wider and flatter cytoplasm of $3T3^{\Delta\gamma1}$-1 cells. (**B**) Cell spreading on FN. Cells were maintained in suspension for 30 min, and then plated on FN. At the intervals indicated, cells were reacted with FITC–phalloidin to detect filamentous actin. (**C**) Decay of the elaborate actin network resulting from OA treatment. $3T3^{\Delta\gamma1}$-1 cells were maintained in suspension for 30 min, and then plated on FN, when OA or diluent (DMSO) was added at the concentrations indicated. After 1 h, cells were stained with TRITC–phalloidin. (**D**) Nascent FA. Cells were maintained in suspension for 30 min, and then plated on FN. One hour later, cells were reacted with paxillin (Pax), vinculin (Vin) or FAK Ab. Cells are shown at the same magnification in (B), (C) and (D). (**E**) Quantitative demonstration of the immunostain in (D). The immunostain spikes for paxillin, vinculin and FAK were counted for each cell using IPLab spectrum software. The data represent the mean values (± SE) by scoring at least 20 cells per clone and pooling the data from three experiments. *P <0.05 by t-test when compared with the values of paxillin immunostain in 3T3 and $3T3^{\gamma1}$ cells.

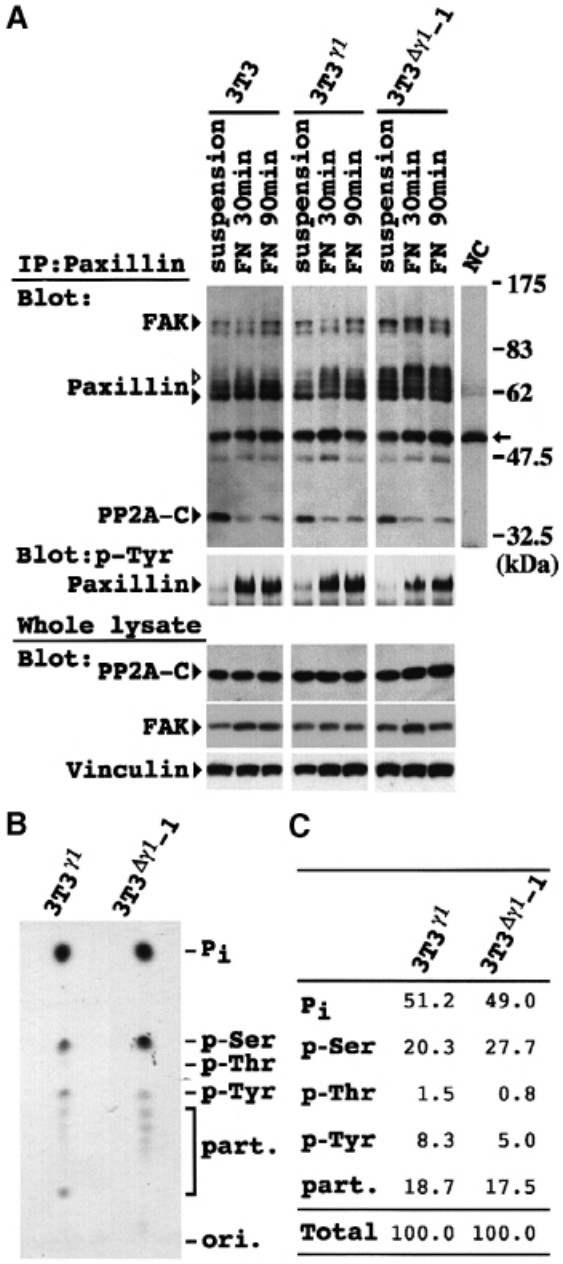

Fig. 5. Enhanced paxillin phosphorylation on serine residues in 3T3$^{\Delta\gamma1}$ cells. (**A**) Cells were lysed at 30 min after non-adherent culture (suspension), and 30 (FN 30min) and 90 (FN 90min) min after plating on FN. Immunoprecipitates with paxillin mAb (upper and center panels) and whole-cell lysates (lower panels) were separated by SDS–PAGE. The blots of immunoprecipitates were probed with a mixture of antibodies against FAK, paxillin (mAb) and PP2A C subunit (upper panel), or anti-phosphotyrosine Ab alone (4G10, center panel). Protein expression in the whole-cell lysates was also examined with antibodies against PP2A C subunit, FAK and vinculin (lower panels). NC indicates a representative result of negative controls. White and black arrowheads beside paxillin indicate phosphorylated and unphosphorylated paxillin, respectively. The arrow on the right indicates the position of the IgG heavy chain. (**B**) Phosphoamino acid analysis of 3T3$^{\gamma1}$ and 3T3$^{\Delta\gamma1}$-1 cells. Immunoprecipitated paxillin with a radioactivity of 500 c.p.m. was hydrolyzed and loaded onto a thin-layer chromatography plate. Co-migration of ninhydrin-stained phosphoamino acid standards is indicated on the right. P_i indicates the position of free ^{32}P-labeled inorganic phosphate. Lower spots are partial hydrolysis products (part.). (**C**) Quantification of phosphorylation on serine, threonine and tyrosine residues. Signal intensity for each residue, P_i or partial hydrolysis products in (B) was quantified and expressed as a percentage of the total intensity.

threonine residues in 3T3$^{\Delta\gamma1}$-1 cells (Figure 5B). This was also the case in 3T3$^{\gamma1}$ cells, but the degree of serine phosphorylation was significantly higher in 3T3$^{\Delta\gamma1}$-1 cells. On the contrary, tyrosine residues were less phosphorylated in 3T3$^{\Delta\gamma1}$-1 cells (Figure 5C). These results indicated that enhanced paxillin phosphorylation in 3T3$^{\Delta\gamma1}$-1 cells occurred on the serine residues but not on the tyrosine or threonine residues.

Co-localization of Δγ1 with paxillin

We also found that a portion of the PP2A C subunit content of these cells was co-immunoprecipitated with paxillin Ab (Figure 5A). FAK was also present in the complex (Figure 5A). Reciprocally, a portion of the paxillin content of the lysates was co-immunoprecipitated with PP2A C subunit Ab (Figure 6A). The extent of association between paxillin and PP2A C subunit decreased after the cell attachment to FN (Figure 5A). The interaction between paxillin and PR55 regulatory subunit was not detectable by the co-immunoprecipitation (data not shown).

The amounts of the B56γ isoforms and Δγ1 co-immunoprecipitated with PP2A C subunit Ab were correlated with those in the cell lysates (Figure 6A). Despite its relatively high abundance in the cell lysate, B56γ3 was co-immunoprecipitated only weakly with paxillin Ab (Figure 6B). Instead, B56γ2, γ1 and Δγ1 were co-immunoprecipitated preferentially, though B56γ1 and Δγ1 were expressed less (Figure 6B).

To examine the intracellular localization of B56γ isoforms, COS-7 cells were transfected with vectors expressing either hemagglutinin (HA)-tagged full-length B56γ3, γ2, γ1 or Δγ1 (Figure 6C). Both HA-tagged B56γ3 and γ2 proteins showed diffuse cytoplasmic and pronounced nuclear localization. The B56γ3 protein displayed more pronounced nuclear localization. HA-tagged B56γ1 and Δγ1 proteins diffusely stained the cytoplasm rather than the nucleus of COS-7 cells. In addition, both B56γ1 and Δγ1 were localized at or near the cell edge, where they were visualized as green dots (Figure 6C). When the same cells were visualized with Cy3 IF to detect paxillin, the punctate stain for B56γ1 and Δγ1 was found to coincide well with paxillin localization at the FA (Figure 6C). Co-localization was clearly demonstrated in the merged images of Cy2 and Cy3 IF (Figure 6C).

Inhibitory effect of Δγ1 on the dephosphorylation of paxillin by PP2A

To examine whether the PP2A heterotrimer containing Δγ1 would cause paxillin hyperphosphorylation in 3T3$^{\Delta\gamma1}$-1 cells, an *in vitro* phosphatase assay was performed. Either calf intestinal alkaline phosphatase (CIAP) or PP2A AC dimer rapidly erased the retarded band corresponding to hyperphosphorylated paxillin in 3T3$^{\Delta\gamma1}$-1 cells (Figure 7A). Since all the B56γ normal isoforms as well as Δγ1 were present in the cell lysate, it seemed difficult to determine the effect of Δγ1 on PP2A activity under these conditions. Hence, hyperphosphorylated paxillin free from associated partner molecules including the various B56 isoforms was obtained and incubated with various forms of the PP2A AC dimer or heterotrimers (Figure 7B). Instead of promoting dephosphorylation of paxillin, the AC dimer mixtures containing B56γ2 and γ1

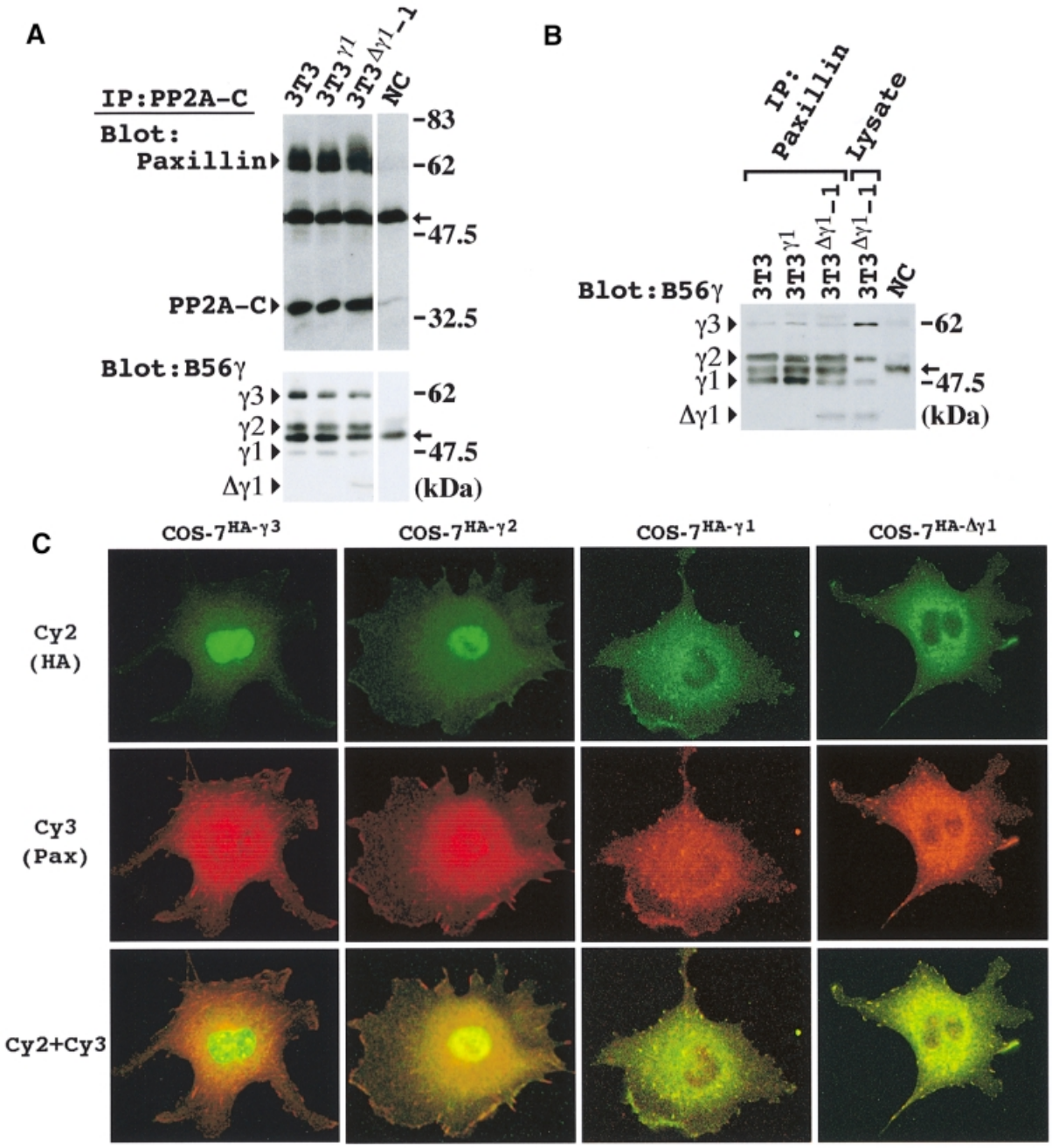

Fig. 6. Co-localization of Δγ1 with paxillin. (**A**) Co-immunoprecipitation of paxillin and PP2A B56γ isoforms by PP2A C subunit Ab. Cells were lysed 30 min after non-adherent cell cultivation and immunoprecipitated with PP2A C subunit Ab. The blot was probed with a mixture of paxillin (mAb) and PP2A C antibodies (upper panel), or B56γ Ab alone (lower panel). (**B**) Cells were lysed 30 min after being plated on FN, and immunoprecipitated with paxillin mAb. The immunoprecipitates and whole-cell lysate (50 μg) of $3T3^{\Delta\gamma1}$-1 cells were blotted and probed with anti-B56γ Ab. The positions of the B56γ isoforms, γ3, γ2, γ1 and Δγ1, are indicated on the left of the blots in (A) and (B). NC indicates a representative result of negative controls in (A) and (B). Arrows in (A) and (B) indicate the position of the IgG heavy chain. (**C**) Subcellular localization of HA-tagged B56γ3, γ2, γ1 and Δγ1 proteins. COS-7 cells were transiently transfected with HA-tagged full length B56γ3 ($COS\text{-}7^{HA\text{-}\gamma3}$), γ2 ($COS\text{-}7^{HA\text{-}\gamma2}$), γ1 ($COS\text{-}7^{HA\text{-}\gamma1}$) or Δγ1 ($COS\text{-}7^{HA\text{-}\Delta\gamma1}$) vector. After transfection, cells were replaced on chamber slides, reacted with anti-HA and paxillin polyclonal Ab, and stained with Cy2 (green; upper row) and Cy3 (red; center row), respectively. Cy2 and Cy3 images were merged into one (lower row).

rather delayed paxillin dephosphorylation: the dephosphorylation effect was small at 30 min, but reached a level near that of the AC dimer alone at 60 min (Figure 7B). In contrast, the AC mixture containing Δγ1 showed the smallest effect on paxillin dephosphorylation even at 60 min (Figure 7B). Addition of OA to the reaction resulted in nearly complete inhibition of paxillin dephosphorylation (Figure 7B).

Δγ1 enhanced the invasive phenotype of F10 cells

We introduced either pAP3neo-B56γ1 or pAP3neo-IAP-γ1 into F10 cells, and obtained the three G418-resistant clones, $F10^{\gamma1}$, $F10^{\Delta\gamma1}$-1 and $F10^{\Delta\gamma1}$-2. Δγ1 expression was faintly detectable in the cultured $F10^{\Delta\gamma1}$-1 cells, and increased 5-fold when the cells metastasized into lymph nodes (Figure 8A). Paxillin phosphorylation was slightly enhanced in cultured BL6 and $F10^{\Delta\gamma1}$-1 cells, but the

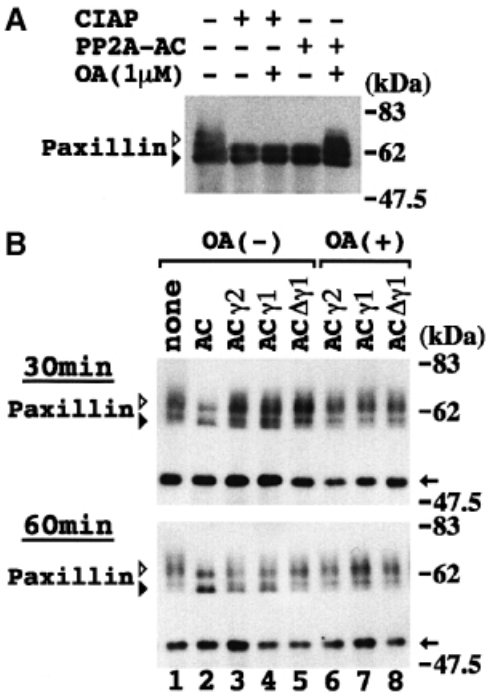

Fig. 7. Inhibitory effect of Δγ1 on PP2A dephosphorylation of paxillin. (**A**) *In vitro* phosphatase assay. 3T3$^{\Delta\gamma1}$-1 cells were lysed in PP2A reaction buffer 30 min after being plated on FN, and incubated with CIAP or the PP2A AC dimer at 30°C for 30 min. The reaction mixture was blotted with paxillin mAb. Addition of OA (1 μM) to the reaction excluded non-specific effects of PP2A. (**B**) *In vitro* paxillin dephosphorylation assay with various PP2A heterotrimers. Hyperphosphorylated paxillin bound to protein G–Sepharose was obtained from 3T3$^{\Delta\gamma1}$-1 cells plated on FN-coated dishes for 30 min. PP2A AC dimer was allowed to bind recombinant B56γ2, γ1 or Δγ1 in PP2A reaction buffer at 4°C overnight. Paxillin was reacted with PP2A dimer or heterotrimers at 30°C for 30 (upper panel) or 60 (lower panel) min. Various forms of PP2A contained in the reaction mixtures are indicated above the panels. In lanes 6, 7 and 8, the reaction mixtures also contained OA (1 μM). In lane 1, no AC dimer mixture was added to the reaction. The reaction mixtures were blotted with paxillin mAb. Arrows on the right indicate the position of the IgG heavy chain. White and black arrowheads indicate phosphorylated and unphosphorylated paxillin, respectively, in (A) and (B).

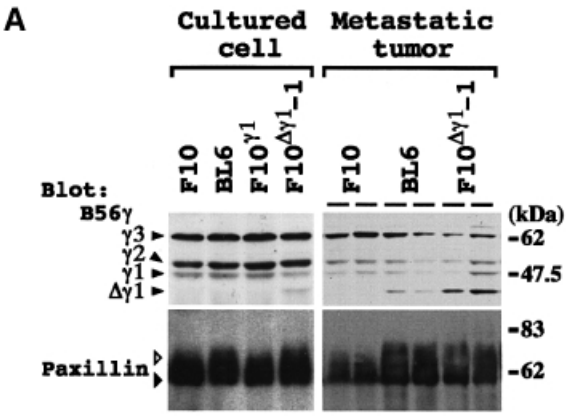

B

Metastasis to the systemic lymph node and lung after subcutaneous injection into the right footpad

Cell	Lymph node				Lung
	Right popliteal	Para-aortic	Right axillary	Left axillary	
F10	8/25(32)	1/25(4)	1/22(5)	0/20(0)	8/20(39)
BL6	5/20(25)	6/20(25)**	2/20(10)	0/20(0)	19/20(95)*
F10$^{\gamma1}$	6/20(30)	0/20(0)	0/20(0)	0/20(0)	6/20(30)
F10$^{\Delta\gamma1}$-1	12/20(55)	2/20(10)	7/20(35)**	1/20(5)	9/21(48)
F10$^{\Delta\gamma1}$-2	6/20(30)	3/20(15)	6/20(30)	0/20(0)	11/20(55)

Fig. 8. The effect of Δγ1 on melanoma cells. (**A**) Correlation of Δγ1 protein expression and enhanced paxillin phosphorylation in melanoma cells. Melanoma cells were cultured under non-adherent conditions for 1 h, lysed and blotted (left column). In the spontaneous metastasis assay, two individual metastatic lesions per clone formed in popliteal lymph nodes were excised, lysed and blotted (right column). The blots were probed with anti-B56γ (upper row) and paxillin (mAb; lower row) antibodies. White and black arrowheads beside paxillin indicate phosphorylated and unphosphorylated paxillin, respectively.
(**B**) Spontaneous metastasis assay. Data are expressed as the number of mice bearing lymph node or lung metastases over the total number of mice. Numbers in parentheses represent the percentage of mice bearing metastases. Metastases to popliteal lymph nodes were documented at amputation, and metastases to the other tissues were documented at autopsy. *P <0.05 by χ^2-test when compared with the values for F10, F10$^{\gamma1}$, F10$^{\Delta\gamma1}$-1 and -2. **P <0.05 by χ^2-test when compared with the values for F10 and F10$^{\gamma1}$. In the lung bearing metastases, BL6 cells produced a significantly larger number of metastatic colonies than F10 cells. The average colony number per mouse was 36.5 for BL6 cells and 2.6 for F10 cells.

enhancement became much more obvious when the cells metastasized into lymph nodes (Figure 8A). Δγ1 expression and paxillin phosphorylation in the F10$^{\Delta\gamma1}$-2 clone were comparable with those of the F10$^{\Delta\gamma1}$-1 clone (data not shown). The metastatic behavior of the melanoma cells was examined (Figure 8B). Lung metastasis was not affected by transfection with B56γ1 or Δγ1. In contrast, F10$^{\Delta\gamma1}$-1 and -2 clones showed a higher incidence of metastasis in the right axillary lymph nodes than did F10 or F10$^{\gamma1}$ cells, and there was a difference in the lymph node region targeted by metastasis of F10$^{\Delta\gamma1}$ clones and BL6 cells.

Discussion

We found that an IAP insertion occurs in one allele of the gene encoding the PP2A B56γ subunit in BL6 cells. From this allele, the IAP–B56γ1 chimeric mRNA was transcribed abundantly in BL6 cells, probably due to strong promoter activity of the IAP LTR sequence. The chimeric mRNA encoded Δγ1. Of note is the fact that Δγ1 was detected only in *in vivo* growing BL6 cells, but not in cultured BL6 cells. The result suggests that the environment for cell growth *in vivo* is quite distinct from that in cell culture, which resulted in the alteration of post-transcriptional regulation. The *in vivo* environment might allow enhanced translation or increased protein stability of Δγ1.

The diversity of the PP2A regulatory subunits suggests specific physiological roles for individual holoenzymes. We found that the PP2A C subunit and B56γ isoforms were associated with paxillin. B56γ2 and γ1 were immunoprecipitated with paxillin in preference to B56γ3. This appeared to be due to the pronounced nuclear localization of B56γ3, which has a bipartite nuclear localization signal in its

C-terminus (McCright *et al*., 1996; Tehrani *et al*., 1996). IF clearly demonstrated that B56γ1, but not B56γ2, co-localized with paxillin at FA. In these experiments, Δγ1 behaved similarly to B56γ1. In addition, Δγ1 did not alter the association between PP2A C subunit and paxillin (Figure 5A). Since PP2A A and C subunits form a dimeric core in cells (Usui *et al*., 1988), B56γ1 and Δγ1 appeared to target the PP2A AC dimer to paxillin at FA.

$3T3^{\Delta\gamma1}$ cells showed an impaired cell cycle checkpoint regulation at G_2/M and an increased cell migration activity. Paxillin phosphorylation was constitutively enhanced in these cells. As might be expected from these results, the Δγ1-containing PP2A heterotrimer was much less effective in dephosphorylating paxillin as compared with the normal PP2A heterotrimers (Figure 7B). Although B56γ1 could direct the AC dimer towards paxillin, the B56γ1-containing PP2A heterotrimer dephosphorylated paxillin less effectively than the AC dimer. This result does not exclude but rather favors a mechanism by which the B56γ1-containing PP2A heterotrimer indirectly regulates paxillin phosphorylation, for example via one of the many protein kinases present in FA.

Constitutive paxillin phosphorylation in $3T3^{\Delta\gamma1}$ cells suggests that association between the Δγ1-containing PP2A heterotrimer and paxillin precedes paxillin localization at FA. Cell adhesion promotes paxillin recruitment from the *trans*-Golgi/endosomal pool into focal contacts. Several paxillin-associated proteins, such as $p95^{PKL}$ and clathrin, were assumed to be involved in this process (Turner *et al*., 1999). Recently, Molloy *et al*. (1998) demonstrated a role for the PP2A-containing PR55 regulatory subunit in regulating protein localization in the *trans*-Golgi/endosomal system. In this regard, it will be important to determine the subcellular localization of B56γ isoforms and Δγ1 in the earlier stages of cell adhesion.

Upon plating on FN, paxillin rapidly localized to nascent FA in $3T3^{\Delta\gamma1}$ cells. Similarly, the phospho-mimetic mutant molecule of paxillin, in which the second serine residue Ser481 of the LIM3 domain was mutated to aspartic acid, was localized efficiently to nascent FA (Brown *et al*., 1998). Paxillin is phosphorylated rapidly and mainly on serine residues during macrophage adhesion to vitronectin and fibroblast adhesion to FN (De Nichilo and Yamada, 1996; Bellis *et al*., 1997). Paxillin phosphorylation on serine residues appeared to be required for paxillin recruitment into focal contacts, especially during the early phase of cell adhesion.

Rapid recruitment of paxillin into FA was coupled with formation of a well-organized actin stress fiber network. Once localized at nascent FA, paxillin serves a multi-domain adaptor function at these sites. By virtue of this function, assembly of molecules necessary for the establishment of FA seemed to proceed efficiently. Turner *et al*. (1999) demonstrated a role for paxillin as an adaptor molecule in cell spreading, which is mediated through the LD4 motif. Δγ1 was implicated in increased cell migration. To migrate, cells need to reorganize their cytoskeletons under spatial and temporal regulation. The first step of migration is unidirectional extension of filopodia and lamellipodia, which has been assumed to share a common molecular mechanism with that of cell spreading (Price *et al*., 1998). Rapid recruitment of paxillin into FA might promote this process.

Increased cell migration and a well-developed cytoskeleton are characteristic properties of several types of highly invasive tumor cells (Verschueren *et al*., 1994; Malliri *et al*., 1998). Indeed, Δγ1 rendered F10 cells as invasive as BL6 cells in lymph node metastasis. Tumor cell–extracellular matrix interaction modulates the ability of tumor cells to achieve lymph node metastasis (Nip *et al*., 1992; Tawil *et al*., 1996). Prompt cytoskeletal reorganization and cell spreading in response to extracellular matrix may be of primary importance for the initiation of tumor invasion. Currently, a complex containing paxillin and PKCμ, a serine kinase, has been shown to be formed in highly metastatic cancer cell invadopodia, actin-containing protrusions extending into the matrix (Bowden *et al*., 1999). Paxillin may be involved in invadopodia formation and extension under the control of its phosphorylation state by PKCμ.

PP2A, as well as PP1, has been postulated to limit tumor motility (Young *et al*., 1993). This suggestion came from the observation that OA rendered tumor cells more motile (Maier *et al*., 1995). However, the precise mechanism of PP2A involvement in this process has been unclear. We have provided a clue to explore the relationship in tumor cells between PP2A insufficiency and malignant progression. Among a variety of regulatory subunit isoforms of PP2A, one mutation in one isoform might lead to the acquisition of more malignant phenotypes. Since Δγ1 was potent for the targeting of PP2A to paxillin, insufficient activity of the Δγ1-containing PP2A heterotrimer could cause distinct cellular events such as adhesion, spreading, migration and invasion, all of which are characteristic features of malignant cells.

Materials and methods

Isolation of cDNA and genomic clones

F10 and BL6 cDNA libraries and the subtracted library were constructed with pAP3neo vector according to methods described (Ito *et al*., 1998; Kobori *et al*., 1998). After four rounds of subtraction, ~1500 clones were rescued and subjected to Northern blot analysis. The DNA sequences were used to search the htgs database using the BLASTN algorithm. From the BL6 cDNA library, plasmids containing the full-length forms of B56γ3 (pAP3neo-B56γ3), γ2 (pAP3neo-B56γ2), γ1 (pAP3neo-B56γ1) and Δγ1 (pAP3neo-IAP-γ1) were obtained. The chimeric cDNA sequence of pAP3neo-IAP-γ1 had been reported in DDBJ/EMBL/GenBank (accession No. U59418), but lacked 54 nucleotides at the 5′ end. A BL6 genomic library was constructed using a Lambda Dash II/*Bam*HI vector kit (Stratagene). The sequence data of the B56γ locus were submitted to DDBJ/EMBL/GenBank (accession No. AB026817).

Cell culture and transfection

B16 melanoma cells and sublines were kindly provided by Dr I.J.Fidler (University of Texas). 3T3 and COS-7 cells were purchased from ATCC. All cells were maintained in Dulbecco's modified Eagle's medium (DMEM) with 10% fetal calf serum (FCS). Bacterial grade dishes (Becton Dickinson) were used for non-adherent culture conditions; adherent culture conditions were produced by coating the dishes with FN (10 μg/ml; Gibco-BRL). For cell cycle analysis, cells received 8 Gy of γ-irradiation, and subsequently were cultured for 15 h. Cells were analyzed by FACScan (Becton Dickinson) as described (Kawabe *et al*., 1997). For the *in vitro* migration assay, blind well chambers (96-well; Nuclepore, Pleasanton, CA) were used, and conditioned medium was prepared by overnight culture of 3T3 cells in DMEM with 0.1% bovine serum albumin (BSA). The lower wells were filled with conditioned medium and the upper wells were filled with DMEM plus 0.1% BSA containing 5×10^3 cells. Some upper wells also contained OA (100 nM). After 4 h of incubation, cells migrating through polycarbonate membrane (8.0 μm pore size; Nuclepore) from the upper to the lower wells were

counted. 3T3 and F10 cells were stably transfected with pAP3neo-B56γ1 and pAP3neo-B56Δγ1 by resistance to G418 (1.5 mg/ml). For transient transfection, a mixture containing 3 μl of FuGENE™ 6 (Boehringer Mannheim) and 1 μg of plasmid DNA was added to COS-7 cell culture in 35 mm dishes, and incubated overnight.

Northern and RT–PCR analysis

Using the standard method, Northern blot analysis was performed. Relative signal intensity was calculated with the BAS 2000 system (Fuji, Japan). RT–PCR analysis was performed as described (Ito *et al*., 1998), using the following primers (see also Figure 1B): sense: F#1, 5′-AGGATGGTGGTGGATGCGG-3′; F#2, 5′-GCAGGAGGGATACTTCATTC-3′; and F#3, 5′-CCACCTTCCTCCAATCCCAC-3′; antisense: R#1, 5′-TTCCAGTAATAGAGCGCCCG-3′; R#2, 5′-CACTCCCGAGTTACTCTCTT-3′; and R#3, 5′-CTCGGACTTGCGGAGTGCAAGAGG-3′.

In vitro transcription/translation

Using the TNT T7 quick coupled transcription/translation system (Promega), the indicated plasmids were transcribed and translated with [^{35}S]methionine.

Plasmid construction

Using pAP3neo-B56γ1 as a template, PCR was carried out with two sense primers (F-Asc-1 and 2) containing an *Asc*I site and one antisense primer (R#2 in Figure 1B): F-Asc-1, 5′-CATGGCGCGCCGAGGATGGTGGTGGATGCGG-3′; F-Asc-2, 5′-CATGGCGCGCCGATGGTGGAGTATATCACCC-3′. A set of primers, F-Asc-1 and R#2, amplified the 5′ portion common to B56γ3, γ2 and γ1 cDNA, and another set of primers, F-Asc-2 and R#2, amplified the 5′ portion of Δγ1 cDNA. The PCR-amplified DNA fragments were treated with Klenow DNA polymerase and then with *Eco*RI. Plasmid constructs pAP3neo-B56γ3, B56γ2, B56γ1 and IAP-Δγ1 were treated by *Mlu*I, Klenow DNA polymerase and *Eco*RI, in this order, to obtain linearized plasmid constructs lacking the 5′ portion of B56γ cDNA. The resulting plasmid constructs were ligated with the PCR-amplified DNA fragments that had been blunt-ended at their 5′ ends and contained the *Eco*RI site at their 3′ ends. The in-frame *Asc*I–*Not*I (the *Not*I site is located in the multicloning site of pAP3neo) cDNA fragments for B56γ isoforms were used as inserts for ligation with epitope-tagged plasmid vector, which was subjected to the following modifications. We generated a DNA fragment carrying the entire open reading of HA along with an *Eco*RI site at the 5′ end and *Asc*I plus *Eco*RV sites at the 3′ end (sense strand: 5′-AATTCATGTACCCATACGATGTTCCTGACTATGCGGGCGCGCCGAT-3′). This DNA fragment was inserted into the pcDNA3 vector (Invtrogen) via *Eco*RI–*Eco*RV sites. A synthetic linker carrying an *Asc*I site (GATCCGGCGCGCCG) was inserted into the *Bam*HI site of the pGEX4T-2 vector (Pharmacia). These modifications allowed the cDNA inserts to be fused in-frame via *Asc*I–*Not*I sites.

Antibodies

The modified pGEX4T-2 vector encoding the GST-B56γ2, γ1 and Δγ1 fusion proteins was introduced into *Escherichia coli* ADA202. After induction by 0.2 mM isopropyl-β-D-thiogalactopyranoside (IPTG) for 4 h, GST fusion proteins were purified from *E.coli* lysates by reduced glutathione–Sepharose (Pharmacia). Rabbits were immunized by standard protocols. The IgG fractions were purified by passing sera through affinity columns containing the purified fusion proteins. Among the three antisera obtained, antiserum against recombinant B56γ1 recognized the B56γ normal isoforms and Δγ1 with the smallest background: this antiserum was termed anti-B56γ Ab.

Other primary antibodies were: paxillin (monoclonal Ab, Clone 349; Transduction Laboratories, Lexington, KY), paxillin (polyclonal Ab 199-217; Mazaki *et al*., 1997), PP2A C subunit (Clone 46; Transduction Laboratories), PP2A PR55 subunit (C-20; Santa Cruz Biotechnology), FAK (Clone 77; Transduction Laboratories), vinculin (VIN-11-5; Sigma), HA (Clone 16B12; Berkeley Ab Co., Richmond, CA), phosphotyrosine (4G10; Upstate Biotechnology, Lake Placid, NY) and PCNA (PC10; Dako, Kyoto, Japan) antibodies. Secondary antibodies were: Cy2-labeled anti-mouse IgG (Jackson ImmunoResearch, West Grove, PA), Cy3-labeled anti-rabbit IgG (Jackson ImmunoResearch), fluorescein isothiocyanate (FITC)-labeled anti-mouse IgG (MBL), peroxidase (POD)-labeled anti-mouse IgG1 (A85-1; Pharmingen, San Diego, CA), POD-labeled anti-rabbit IgG (MBL), POD-labeled anti-goat IgG (MBL) and POD-labeled anti-mouse IgG (Jackson ImmunoResearch) antibodies.

IP and Western blot analysis

In most cases, cells and tumor tissues were lysed in a buffer containing 10 mM Tris–HCl pH 8.0, 1 mM EDTA, 0.5% NP-40, 1 mM phenylmethylsulfonyl fluoride (PMSF), 0.1 mM Na_3VO_4 and 0.1 mM NaF. Otherwise, cells were lysed in RIPA buffer (50 mM Tris–HCl pH 7.5, 150 mM NaCl, 1% NP-40, 0.1% SDS, 0.5% sodium deoxycholate, 1 mM PMSF, 0.1 mM Na_3VO_4 and 0.1 mM NaF). For IP, 250 μg of lysates were incubated with 2.5 μg of the paxillin (mAb) or PP2A C subunit Ab, and precipitated with protein G–Sepharose (Pharmacia). The immunoprecipitates, total cell or tissue lysates (50 μg per lane), were separated on 10% SDS–polyacrylamide gels, transferred to Immobilon (Millipore) and reacted with primary and POD-labeled secondary antibodies. Blots were reacted with Renaissance reagents (NEN, Boston, MA) before exposure. For a negative control, every cell lysate was immunoprecipitated with 2.5 μg of mouse control IgG1, κ (MOPC-21, Sigma): every lysate yielded a similar result.

PP2A plus PP1 phosphatase activity

The phosphatase activity of cells lysates on phosphorylase *a* (Sigma) was measured as described (Cohen *et al*., 1988).

In vitro CIAP and PP2A assay

Whole-cell lysates (50 μg) were prepared in PP2A reaction buffer [20 mM HEPES pH 7.0, 1 mM dithiothreitol (DTT), 1 mM $MnCl_2$, 100 μg/ml BSA, 50 μM leupeptin] and incubated with CIAP (3 U; Takara, Ohtsu, Japan) or PP2A AC dimer (0.02 U; Upstate Biotechnology) at 30°C for 30 min in the presence or absence of OA. The reaction was terminated by adding 4× SDS sample buffer (0.4 M Tris–HCl pH 6.8, 8% SDS, 20% glycerol, 10% 2-mercaptoethanol, 0.2% bromophenol blue).

To prepare PP2A heterotrimers, recombinant B56γ2, γ1 and Δγ1 proteins were eluted in 50 mM Tris–HCl pH 8.0, 10 mM glutathione and 20% glycerol at a concentration of 2.0 mg/ml. PP2A AC dimer and the recombinant proteins (at a molar 1:10 ratio) were incubated together in PP2A buffer at 4°C overnight, and used as B56γ isoform-containing PP2A heterotrimers. Phosphorylated paxillin was prepared as follows: 30 min after 3T3$^{\Delta\gamma1}$-1 cells were plated on FN-coated dishes, cells were lysed in RIPA buffer and immunoprecipitated with paxillin mAb and protein G–Sepharose. Paxillin bound to protein G–Sepharose was washed extensively with PP2A buffer and divided into aliquots. Each aliquot was incubated with either the PP2A AC dimer (0.02 U) or the PP2A AC (0.02 U)–B56γ mixtures at 30°C for the indicated time in the presence or absence of OA. The reaction was terminated by adding SDS sample buffer. The samples were separated on an SDS–polyacrylamide gel and blotted with paxillin mAb.

Phosphoamino acid analysis

Logarithmically growing cells (3×10^6) were incubated in phosphate-free DMEM (Gibco-BRL) with 10% dialyzed FCS for 30 min, and then labeled with 1 mCi/ml [^{32}P]orthophosphate (carrier free; Amersham) for 4 h in phosphate-free DMEM with 5% dialyzed FCS. Cells were lysed in RIPA buffer and immunoprecipitated with paxillin mAb. The following procedures were according to standard protocols. Relative signal intensity was calculated with the BAS 2000 system.

IF

Cells were plated on FN-coated chamber culture slides (Becton Dickinson) in DMEM plus 0.1% BSA. Cells were fixed at intervals with 3.7% paraformaldehyde in PBS, permeabilized with 0.1% Triton X-100 in PBS, blocked with 2% BSA in PBS, incubated with paxillin (mAb), vinculin and FAK Ab, and stained with FITC-labeled anti-mouse IgG. To detect filamentous actin, cells were incubated with FITC– or tetramethylrhodamine isothiocyanate (TRITC)–phalloidin (Sigma) after blocking. Cells were observed through an Axioplan2 microscope (Carl Zeiss) equipped for epifluorescence. For quantitative analysis, images were collected using IPLab Spectrum software (Scanalytics, Fairfax, VA). Positive immunostaining took the form of a spike in shape. The numbers of spikes in FA were counted for each cell, and quantified by scoring at least 20 cells per clone and pooling the data from three experiments. HA-tagged plasmid-transfected COS-7 cells were replaced on chamber culture slides (Becton Dickinson) in DMEM plus 10% FCS. Next day, cells were treated with the above procedures, reacted with anti-HA Ab and paxillin polyclonal Ab, and stained with Cy2-labeled anti-mouse IgG Ab and Cy3-labeled anti-rabbit IgG Ab, respectively. Cells were visualized using a confocal laser scanning microscope (model 510, Carl Zeiss).

Spontaneous metastasis assay

Individual mice were inoculated with 2.5×10^5 cells, and then treated according to the method described (Poste *et al*., 1980). The metastatic lung colonies were counted macroscopically. Lymph nodes were diagnosed histologically.

Acknowledgements

We thank Mr M.Sakai and Dr S.Okamoto (Osaka Teishin Hospital) for FACScan analysis, and Mr N.Yabuta (Osaka University) for plasmid preparation. This work was supported by a Grant-in-aid for Scientific Research on Priority Areas from the Ministry of Education, Science, Sports and Culture of Japan and a grant from the Osaka Cancer Society.

References

Alessi,D.R., Gomez,N., Moorheah,G., Lewis,T., Keyse,S.M. and Cohen,P. (1995) Inactivation of p42 MAP kinase by protein phosphatase 2A and a protein tyrosine phosphatase, but not CL100, in various cell lines. *Curr. Biol.*, **5**, 283–295.

Bellis,S.L., Perrotta,J.A., Curtis,M.S. and Turner,C.E. (1997) Adhesion of fibroblasts to fibronectin stimulates both serine and tyrosine phosphorylation of paxillin. *Biochem. J.*, **325**, 375–381.

Bowden,U.T., Marth,M., Thomas,D., Glazer,R.I. and Mueller,S.C. (1999) An invasion-related complex of cortactin, paxillin and PKCμ associates with invadopodia at sites of extracellular matrix degradation. *Oncogene*, **18**, 4440–4449.

Brown,M.C., Perrotta,J.A. and Turner,C.E. (1996) Identification of LIM3 as the principal determinant of paxillin focal adhesion localization and characterization of a novel motif on paxillin directing vinculin and focal adhesion kinase binding. *J. Cell Biol.*, **135**, 1109–1123.

Brown,M.C., Perrotta,J.A. and Turner,C.E. (1998) Serine and threonine phosphorylation of the paxillin LIM domains regulates paxillin focal adhesion localization and cell adhesion to fibronectin. *Mol. Biol. Cell*, **8**, 1803–1816.

Burridge,K. and Chrzanowska-Wodnicka,M. (1996) Focal adhesions, contractility, and signaling. *Annu. Rev. Cell Dev. Biol.*, **12**, 463–519.

Burridge,K., Turner,C.E. and Romer,L.H. (1992) Tyrosine phosphorylation of paxillin and $pp125^{FAK}$ accompanies cell adhesion to extracellular matrix: a role in cytoskeletal assembly. *J. Cell Biol.*, **119**, 893–903.

Cohen,P., Alemany,S., Hemmings,B.A., Resink,T.J., Stralfors,P. and Tung,H.Y.L. (1988) Protein phosphatase-1 and protein phosphatase-2 from rabbit skeletal muscle. *Methods Enzymol.*, **159**, 390–408.

De Nichilo,M.O. and Yamada,K.M. (1996) Integrin αvβ5-dependent serine phosphorylation of paxillin in cultured human macrophages adherent to vitronectin. *J. Biol. Chem.*, **271**, 11016–11022.

Farve,B., Turowshi,P. and Hemmings,B.A. (1997) Differential inhibition and posttranslational modification of protein phosphatase 1 and 2A in MCF7 cells treated with calyculin-A, okadaic acid, and tautomycin. *J. Biol. Chem.*, **272**, 13856–13863.

Hannigan,G.E., Leung-Hagesteijin,C., Fitz-Gibbon,L., Coppolino,M.G., Redeva,G., Filmus,J., Bell,J.C. and Dedhar,D. (1996) Regulation of cell adhesion and anchorage-dependent growth by a new β_1-integrin-linked protein kinase. *Nature*, **379**, 91–96.

Harden,N., Lee,J., Loh,H.-Y., Tan,I., Leung,T., Manser,E. and Lim,L. (1996) A *Drosophila* homolog of the Rac- and Cdc42-activated serine/threonine kinase PAK is a potential focal adhesion and focal complex protein that colocalized with dynamic actin structures. *Mol. Cell. Biol.*, **16**, 1896–1908.

Ito,A. *et al*. (1998) Systematic method to obtain novel genes that are regulated by *mi* transcription factor: impaired expression of granzyme B and tryptophan hydroxylase in *mi/mi* cultured mast cells. *Blood*, **91**, 3210–3221.

Kawabe,T., Muslin,A.J. and Korsmeyer,S.J. (1997) HOX11 interacts with protein phosphatases PP2A and PP1 and disrupts G_2/M cell-cycle checkpoint. *Nature*, **385**, 454–458.

Kobori,M., Ikeda,Y., Nara,H., Kato,M., Kumegawa,M., Nojima,H. and Kawashima,H. (1998) Large scale isolation of osteoclast-specific genes by an improved method involving the preparation of a subtracted cDNA library. *Genes Cells*, **3**, 459–475.

Kuff,E.L. and Lueders,K.K. (1988) The intracisternal A-particle gene family: structure and functional aspects. *Adv. Cancer Res.*, **51**, 183–276.

Leung,T., Chen,X-O., Manser,E. and Lim,L. (1996) The p160 RhoA-binding kinase ROKα is a member of a kinase family and is involved in the reorganization of the cytoskeleton. *Mol. Cell. Biol.*, **16**, 5313–5327.

Liotta,L.A., Steeg,P.S. and Stetler-Stevenson,W.G. (1991) Cancer metastasis and angiogenesis: an imbalance of positive and negative regulation. *Cell*, **64**, 327–336.

Maier,G.D., Wright,M.A., Lozano,Y., Djordjevic,A., Matthews,J.P. and Young,M.R.I. (1995) Regulation of cytoskeletal organization in tumor cells by protein phosphatases-1 and -2A. *Int. J. Cancer*, **61**, 54–61.

Malliri,A., Symons,M., Hennigan,R.F., Hurlstone,A.F.L., Lamb,R.F. Wheeler,T. and Ozanne,B.W. (1998) The transcription factor AP-1 is required for EGF-induced activation of Rho-like GTPases, cytoskeletal rearrangements, motility, and *in vitro* invasion of A431 cells. *J. Cell Biol.*, **143**, 1087–1099.

Mazaki,Y., Hashimoto,S. and Sabe,H. (1997) Monocyte cells and cancer cells express novel paxillin isoforms with different binding properties to focal adhesion proteins. *J. Biol. Chem.*, **272**, 7437–7444.

McCright,B., Rivers,A.M., Audlin,S. and Virshup,D.M. (1996) The B56 family of protein phosphatase 2A (PP2A) regulatory subunits encodes differentiation-induced phosphoproteins that target PP2A to both nucleus and cytoplasm. *J. Biol. Chem.*, **271**, 22081–22089.

Millward,T.A., Zolnierowicz,S. and Hemmings,B.A. (1999) Regulation of protein kinase cascades by protein phosphatase 2A. *Trends Biochem. Sci.*, **24**, 186–191.

Molloy,S.S., Thomas,L., Kamibayashi,C., Mumby,M.C. and Thomas,G. (1998) Regulation of endosome sorting by a specific PP2A isoform. *J. Cell Biol.*, **142**, 1399–1411.

Nip,J., Shibata,H., Loskutoff,D.J., Cheresh,D.A. and Brodt,P. (1992) Human melanoma cells derived from lymphatic metastases use integrin αvβ3 to adhere to lymph node vitronectin. *J. Clin. Invest.*, **90**, 1406–1413.

Poste,G., Doll,J., Hart,I.R. and Fidler,I.J. (1980) *In vivo* selection of murine B16 melanoma variants with enhanced tissue-invasive properties. *Cancer Res.*, **40**, 1636–1644.

Price,L.S., Leng,J., Schwartz,M.A. and Bokoch,G.M. (1998) Activation of Rac and Cdc42 by integrins mediates cell spreading. *Mol. Biol. Cell*, **9**, 1863–1871.

Sabe,H., Hata,A., Okada,M., Nakagawa,H. and Hanafusa,H. (1994) Analysis of the binding of the Src homology 2 domain of Csk to tyrosine-phosphorylated proteins in the suppression and mitotic activation of c-Src. *Proc. Natl Acad. Sci. USA*, **91**, 3984–3988.

Shenolikar,S. (1994) Protein serine/threonine phosphatases—new avenues for cell regulation. *Annu. Rev. Cell Biol.*, **10**, 55–86.

Sontag,E., Nunbhakdi-Craig,V., Bloom,G.S. and Mumby,M.C. (1995) A novel pool of protein phosphatase 2A is associated with microtubules and is regulated during the cell cycle. *J. Cell Biol.*, **128**, 1131–1144.

Tawil,N.J., Gowri,V., Djoneidi,M., Nip,J., Carbonetto,S. and Brodt,P. (1996) Integrin α3β1 can promote adhesion and spreading of metastatic breast carcinoma cells on the lymph node stroma. *Int. J. Cancer*, **66**, 703–710.

Tehrani,M.A., Mumby,M.C. and Kamibayashi,C. (1996) Identification of a novel phosphatase 2A regulatory subunit highly expressed in muscle. *J. Biol. Chem.*, **271**, 5164–5170.

Turner,C.E. and Miller,J.T. (1994) Primary sequence of paxillin contains putative SH2 and SH3 domain binding motifs and multiple LIM domains: identification of vinculin and pp125FAK binding. *J. Cell Sci.*, **107**, 1583–1591.

Turner,C.E., Brown,M.S., Perrotta,J.A., Riedy,M.C., Nikolopoulos,S.N., McDonald,A.R., Bagrodia,S., Thomas,S. and Leventhal,P.S. (1999) Paxillin LD4 motif binds PAK and through a novel 95-kD ankyrin repeat, ARF-GAP protein: a role in cytoskeletal remodeling. *J. Cell Biol.*, **145**, 851–863.

Usui,H., Imazu,M., Tsukamoto,H., Azuma,K. and Takeda,M. (1988) Three distinct forms of type 2A protein phosphatase in human erythrocyte cytosol. *J. Biol. Chem.*, **263**, 3752–3761.

Verschueren,H., Van der Taelen,I., Dewit,J., De Braekeleer,J. and De Baetselier,P. (1994) Metastatic competence of BW5147 T-lymphoma cell lines is correlated with *in vitro* invasiveness, motility and F-actin content. *J. Leukocyte Biol.*, **55**, 552–556.

Wera,S. and Hemmings,B.A. (1995) Serine/threonine protein phosphatases. *Biochem. J.*, **311**, 17–29.

Yamashita,K., Yasuda,H., Pines,J., Yasumoto,K., Nishitani,H., Ohtsubo,M., Hunter,T., Sugimoto,T. and Nishimoto,T. (1990) Okadaic acid, a potent inhibitor of type 1 and type 2A protein phosphatases, activates cdc2/H1 kinase and transiently induces a premature mitosis-like state in BHK21 cells. *EMBO J.*, **9**, 4331–4338.

Young,M.R.I., Lozano,Y., Djorjevic,A. and Maier,G.D. (1993) Protein phosphatases limit tumor motility. *Int. J. Cancer*, **55**, 1036–1041.

Received June 28, 1999; revised and accepted December 10, 1999